20th Australasian Fluid Mechanics Conference
Perth, Australia
5-8 December 2016

Direct Numerical Simulation of a Turbulent Line Plume in a Confined Region

N. George[1], A. Ooi[1], K. Moinuddin[2], G. Thorpe[2], I. Marusic[1] and D. Chung[1]

[1]Department of Mechanical Engineering
The University of Melbourne, Parkville VIC 3010, Australia

[2]Centre for Environmental Safety and Risk Engineering
Victoria University, Victoria 8001, Australia

Abstract

We present direct numerical simulations (DNS) of a turbulent line plume in a confined region with adiabatic side, top and bottom walls. The plume originates from a line heat source of length, L, located at the centre of the bottom wall ($z/H = 0$) and rises until it impinges on the top wall ($z/H = 1$) and spreads laterally to produce a buoyant fluid layer. Since the region is confined, the continuous supply of buoyant fluid forces the layer downwards, until it reaches the bottom wall, where the flow is said to be the asymptotic state (Baines and Turner [1]). Presently, two Reynolds numbers, 3840 and 7680, are selected for plume lengths, $L/H = 1$, 2 and 4, where the Reynolds number of the plume is based on H and the buoyant velocity scale, $F_0^{1/3}$, where F_0 is buoyancy flux per unit length. The current simulations are validated with the analytical model presented by Baines and Turner [1]. The simulations exhibit a slow flapping motion of the confined line plume in the asymptotic state, which precludes a straightforward comparison with Baines and Turner's [1] analytical model. For the purpose of comparison with the analytical model, we adapt the shifting method introduced by Hubner [4], which improves agreement with the analytical model.

Introduction

Baines and Turner [1] first studied the stratification developed by a turbulent plume originated from a local heat source (point or line) in a confined region (figure 1), which is commonly referred to as a 'filling box' problem. They considered a plume generated at the centre of the bottom boundary within the initially uniform confined environment. The plume rises to the upper boundary and spread towards the sidewalls, and form a density interface between the plume outflow and the ambient fluid. The continuous supply of buoyant fluid causes this density interface to move downwards towards the source. The 'filling box' problem appears in many industrial and geophysical fluid flows, for example, in building ventilation (e.g. Hunt *et al* [5]), compartment fires (e.g. Zukoski [11]) and in the oceans (e.g. Killworth and Turner [9]). Most previous studies have focused mainly on the filling box containing a point source of buoyancy, plumes from a line source of buoyancy have received less attention. In this paper, we focus our attention on the direct numerical simulations (DNS) of confined line plumes for comparing the Baines and Turner's [1] analytical model. In the current study, we are interested in investigating the accuracy of the Baines and Turner's [1] analytical model with the help of DNS. We also consider the sensitivity of plume behaviour on plume length (L) for different Reynolds numbers (Re_H).

The 'filling box' Model of Baines and Turner (1969)

In order to validate the 'filling box' model with the present DNS results, we review the theory of Baines and Turner [1]. The 'filling box' model is shown schematically in figure 2 where a line source of buoyancy is located on the bottom wall of a box

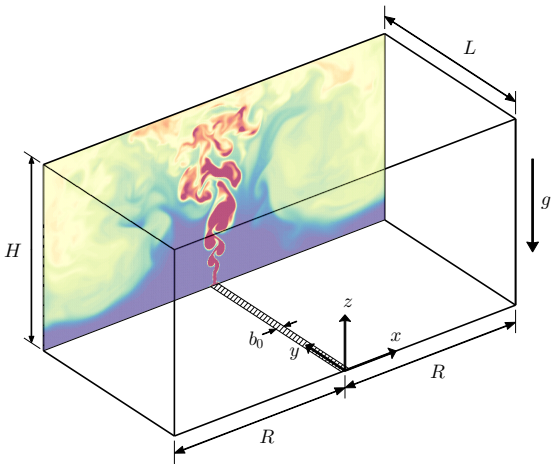

Figure 1: Set up of 'filling box' problem with contours of instantaneous temperature (hot, red and cold, blue) showing a turbulent thermal plume emerging from a line heat source at the centre of the bottom wall. b_0 is the initial plume width (the source width) and g is the acceleration due to gravity.

height H and width $2R$. The source generates a buoyancy flux F_0 per unit length and zero fluxes of volume and momentum. To derive the steady-state solution for turbulent line plume in a confined region, we begin by considering the volume, momentum and buoyancy fluxes for a line plume, which can be derived from the Reynolds averaged momentum equations and continuity equation (see Lee and Emmons [6]). The mean velocity in the vertical direction z is denoted by $\overline{w}$, and in the $x-$direction is denoted by $\overline{u}$. The governing equations for the volume, momentum and buoyancy flux are given by

$$\frac{\mathrm{d}}{\mathrm{d}z}\int_{-\infty}^{+\infty}\overline{w}\,\mathrm{d}x = 2u_e, \tag{1}$$

$$\frac{\mathrm{d}}{\mathrm{d}z}\int_{-\infty}^{+\infty}\overline{w}^2\,\mathrm{d}x = g\beta\int_{-\infty}^{+\infty}(\overline{T}-\overline{T}_\infty)\,\mathrm{d}x, \tag{2}$$

$$\frac{\mathrm{d}}{\mathrm{d}z}\int_{-\infty}^{+\infty}(\overline{T}-\overline{T}_\infty)\,\overline{w}\,\mathrm{d}x = -\int_{-\infty}^{+\infty}\overline{w}\,\frac{\partial\overline{T}_\infty}{\partial z}\,\mathrm{d}x, \tag{3}$$

where u_e is the entrainment velocity ($u_e = \overline{u}|_{x=\pm\infty}$), g is the gravitational acceleration, β is the coefficient of thermal expansion, $\overline{T}$ is the mean temperature and $\overline{T}_\infty$ is the mean environmental temperature. The temperature gradient in the environment is taken into account in the buoyancy flux equation (3), which can be expressed in terms of environmental buoyancy gradient, $\partial\Delta_0/\partial z = g\beta\partial\overline{T}_\infty/\partial z$. Here, the mean vertical velocity ($\overline{w}$) and reduced gravity are approximated by a Gaussian form, i.e. $\overline{w} = w_m\exp(-x^2/b^2)$ and $g\beta(\overline{T}-\overline{T}_\infty) = \Delta\exp(-x^2/b^2)$, where $b(z)$ is the Gaussian plume width, $w_m(z)$

and $\Delta(z)$ are mean vertical velocity and reduced gravity on the geometrical plume centreline, respectively. Gaussian profiles of equal width have been assumed for the vertical velocity and reduced gravity fields in the plume.

As suggested by Morton, Taylor and Turner [8], the rate at which fluid is entrained into the plume is taken as proportional to the mean vertical velocity on the axis of the plume, $u_e = \alpha w_m$, where α is the entrainment coefficient.

The plume equations described above are valid for the line plumes in unconfined environments. (e.g. Lee and Emmons [6]; Pillat and Kaminski [7]). In the case of confined plumes, two other equations are considered for describing the environmental flow parameters. The conservation of mass in the 'filling box' can be written as

$$\sqrt{\pi} b w_m = -2RU \tag{4}$$

where U is the downward velocity of the environment and $2R$ is the width of the box (figure 2), and the development of the buoyancy field in the environment is governed by

$$\frac{\partial \Delta_0}{\partial t} = -U \frac{\partial \Delta_0}{\partial z}. \tag{5}$$

When the buoyant fluid first impinges on the upper boundary

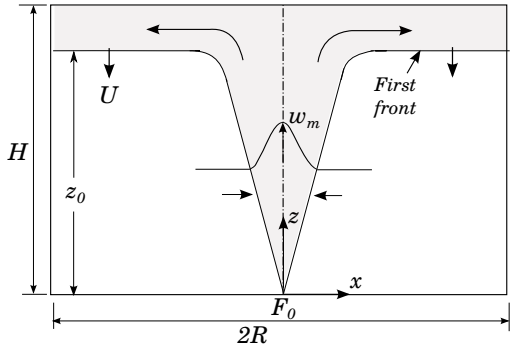

Figure 2: Schematic diagram of the 'filling box' model.

of the confined box, a horizontal thin buoyant layer is formed and then proceeding downwards. The dynamics of horizontal spreading-out flow is ignored. The interface between the buoyant fluid and the ambient fluid is referred as the first front. After this layer reaches the bottom wall, the flow is said to be in the asymptotic state (Baines and Turner [1]). In the asymptotic state, the buoyancy at every point increases linearly with time and the velocity fields are statistically steady. The solution of five equations (three plume equations and two describing the environment) are non-dimensionalized by

$$\begin{aligned}
\Delta_0 &= 2^{-1} F_0^{\frac{2}{3}} \alpha^{-\frac{2}{3}} H^{-1} [f_0(z/H) - \tau], \\
\Delta &= 2^{-\frac{1}{2}} F_0^{\frac{2}{3}} \alpha^{-\frac{2}{3}} H^{-1} f(z/H), \\
w_m &= F_0^{\frac{1}{3}} \alpha^{-\frac{1}{3}} g(z/H), \\
b &= 2\pi^{-\frac{1}{2}} \alpha H h(z/H), \\
U &= F_0^{\frac{1}{3}} \alpha^{\frac{2}{3}} (H/R) j(z/H),
\end{aligned} \tag{6}$$

where, $\tau = F_0^{1/3} \alpha^{2/3} R^{-1} t$. (Note: The above equations are slightly different from Baines and Turner [1], because they are not considered 2 in RHS of volume flux equation (1)).

Set-up of Direct Numerical Simulations

We employ direct numerical simulation to solve the equations of mass, momentum and temperature within the Boussinesq approximation. The resulting governing equations are:

$$\begin{aligned}
&\frac{\partial u_i}{\partial t} + u_j \frac{\partial u_i}{\partial x_j} = -\frac{1}{\rho} \frac{\partial p}{\partial x_i} + \nu \frac{\partial^2 u_i}{\partial x_j^2} + g\beta T \delta_{i3}, \\
&\frac{\partial T}{\partial t} + u_j \frac{\partial T}{\partial x_j} = \kappa \frac{\partial^2 T}{\partial x_j^2}, \qquad \frac{\partial u_i}{\partial x_i} = 0,
\end{aligned} \tag{7}$$

where ν is the kinematic viscosity, g is the gravitational acceleration, β is the coefficient of thermal expansion and κ is the thermal diffusivity.

A line temperature flux source (f_w) along the $y-$direction is maintained at the bottom wall. The distribution of temperature flux is set as Gaussian, $f_w = -\kappa A \exp(-x^2/b_0^2)$, where κA is the maximum temperature flux. The buoyancy flux per unit length (F_0) is computed by integrating temperature flux along the $x-$direction

$$F_0 = \sqrt{\pi} g \beta \kappa A b_0. \tag{8}$$

The dimensionless parameters governing the present simulations are Reynolds number,

$$Re_H = F_0^{1/3} H/\nu \tag{9}$$

and Prandtl number, $Pr = \nu/\kappa$, which is set as 0.71. We have selected two different Reynolds numbers, 3840 and 7680 for plume lengths, $L/H = 1, 2,$ and 4 (table 1). The asymptotic state is calculated by measuring the advancement of the temperature interface near the side wall as a function of time. After the asymptotic state is reached, mean statistics are computed by averaging over at least 150 non-dimensional time units at the interval of 0.9. The governing equations are solved using the code described in Ng *et al*. [3].

The bottom, top, left, and right boundaries are no-slip and no-penetration walls. Periodic boundary conditions are imposed on velocity(v), pressure (p) and temperature (T) in the $y-$direction. In the present case, we set all initial velocities to zero and added a random perturbation to the temperature field in a semi-circular prism region, $x^2 + z^2 < (2b_0)^2$ located near the plume, in order to trigger a transition in the rising plume before it reaches the top wall. The magnitude of perturbations added to the flow is based on $(g\beta\Delta T b_T)^{1/2} b_0/\nu = 3.77$, and is kept constant for all simulations.

The grid spacing is uniform in the x, y and $z-$directions. The resolutions of the present simulations are kept constant relative to $F_0^{1/3}$ and ν. We compute the resolutions based on the Kolmogorov length scale, $\eta = (\nu^3/\bar{\varepsilon})^{1/4}$, where $\bar{\varepsilon} = 15\nu\overline{(\partial w'/\partial z)^2}_{x=0}$ is the turbulent dissipation along the plume centre line. The initial Gaussian plume width (b_0) is calculated based on the ratio of Gaussian width of temperature gradient distribution, which we imposed on the bottom wall of the box, to the grid spacing in the x-direction. The ratio, $b_0/\Delta x$ is fixed as 3.2 to ensure 6 grid points on both sides of the Gaussian curve in order to ensure the numerical stability of the code. The value of b_0 is maintained as small as possible to approximate a line temperature source.

In the present simulation, the domain size, (L_x, L_y, L_z), the number of grid points in all directions (N_x, N_y, N_z) and the kinematic viscosity (ν) are arbitrarily chosen as in a physical experiment. Given the number of grid points, $\Delta x = \Delta y = \Delta z$ is then determined. The value of b_0, η and F_0 are obtained by setting

Re_H	H/R	L/H	n_x	n_y	n_z	$\Delta x F_0^{1/3}/\nu$	$\Delta y F_0^{1/3}/\nu$	$\Delta z F_0^{1/3}/\nu$	$t_{start} F_0^{1/3}/H$	$t_{end} F_0^{1/3}/H$
3840	1	1	256	128	128	30.0	30.0	30.0	31	256
3840	1	2	256	256	128	30.0	30.0	30.0	30	256
3840	1	4	256	512	128	30.0	30.0	30.0	30	282
7680	1	1	512	256	256	30.0	30.0	30.0	28	203
7680	1	2	512	512	256	30.0	30.0	30.0	27	152
7680	1	4	512	1024	256	30.0	30.0	30.0	26	157

Table 1: Simulation parameters of the present cases.

$b_0/\Delta x = 3.2$, $\Delta x/\eta \approx 3$ and $\eta F_0^{1/3}/\nu = 10$, which can then be substituted in (8) to obtain $g\beta A$.

Plume Centreline Alignment

In the present simulation, we observed that the plume dynamical centreline was deviating from its geometrical centreline in the asymptotic state (Figure 3(a) and (b)). This centreline deviation is due to the flapping motion of the plume and its meandering along the $y-$direction. Cetegen *et al* [2] experimentally studied the oscillatory behaviour of line plumes in an open environment. This kind of dynamic behaviour affects the steady-state characteristics of line plumes, which precludes a straightforward comparison with the analytical model. Therefore, we introduce a shifting technique for the lateral displacement of dynamical plume centreline (Figure 3(c)), which was originally developed by Hubner [4]. The flow properties can thus be defined based on dynamical plume centreline coordinate system

$$(\cdot)_s(x_s,y,z,t) = (\cdot)(x = x_s + s(y,z,t), y, z, t). \tag{10}$$

Here x_s is the horizontal coordinate of plume dynamical centreline and s is the deviation of dynamical centre from the geometrical centre (Figure 3(c)). Here, the dynamical centreline is defined as the location of the maximum vertical velocity (w). In order to determine the peak location of vertical velocity(w), we used a low-pass spectral cut-off filter along $y-$direction with a cut-off wavelength of $\lambda_c = 0.5H$. In other words, Fourier coefficients greater than λ_c are set to zero, and then performing an inverse Fourier transformation to obtain the smooth velocity ($\widetilde{w}$). We then identified the deviation of the dynamical plume centre from the geometrical centre at all vertical locations and shifted the dynamical plume centre in Fourier space. After that we calculated the $y-$line average and temporal, which is defined as,

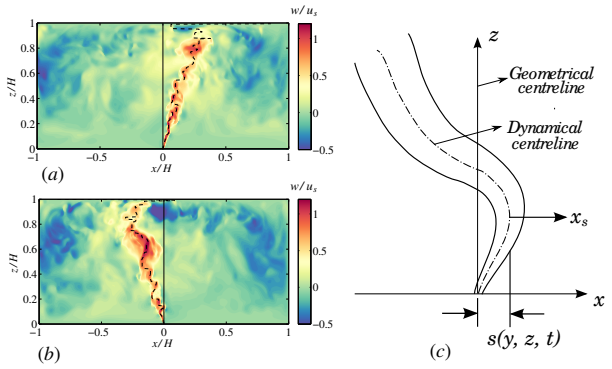

Figure 3: Flapping motion of confined line plume. (a) Vertical velocity contour for $Re_H = 7680$ and $L/H = 4$ at $t/(H/F_0^{1/3}) \approx 100$ at $y/H = 1$, (b) $y/H = 2$ and (c) schematic diagram of the flapping plume.

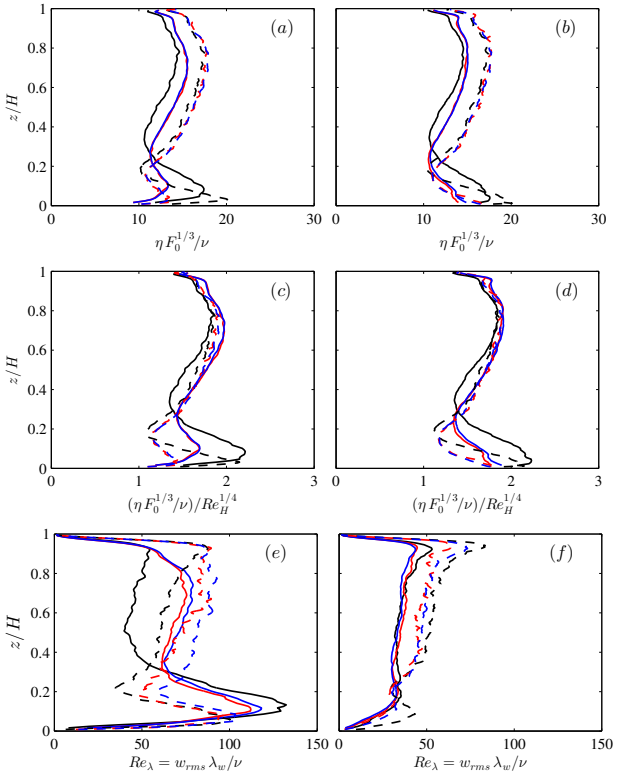

Figure 4: Comparison of Kolmogorov and Taylor micro scale for non-shifted cases (a, c, e) at the geometrical centreline and shifted cases (b, d, f) at the dynamical centreline for different Re_H and L/H: ——, $Re_H = 3840(\ L/H = 1)$; ——, $Re_H = 3840\ (L/H = 2)$; ——, $Re_H = 3840\ (L/H = 4)$; - - -, $Re_H = 7680\ (L/H = 1)$; - - -, $Re_H = 7680\ (L/H = 2)$; - - -, $Re_H = 7680\ (L/H = 4)$.

$$\overline{(\cdot)} = \frac{1}{N}\sum_{n=1}^{N}\frac{1}{L}\int_0^L (\cdot)(y,t_n)\,\mathrm{d}y. \tag{11}$$

To find the mean vertical velocity variance ($\overline{w'^2}$), we decompose the vertical velocity into a mean part and a fluctuating part in time and space,

$$w_s(x_s,y,z,t) = \overline{w}_s(x_s,z) + w'_s(x_s,y,z,t), \tag{12}$$

$$w_s(x_s,y,z,t) = \widetilde{w}_s(x_s,y,z,t) + w''_s(x_s,y,z,t), \tag{13}$$

where w'_s and w''_s are the fluctuations in time and space (y-direction), respectively. From the above two equations, we can calculate the mean w variance as,

$$\overline{w'^2_s} = \overline{[\widetilde{w}_s - \overline{w}_s]^2} + \overline{w''^2_s}. \tag{14}$$

Similarly we can define the straight forward (non-shifted) equation for finding the mean variance as,

$$\overline{w'^2} = \overline{[\widetilde{w} - \overline{w}]^2} + \overline{w''^2}. \quad (15)$$

Results and Discussion

Figure 4 shows the variation of Kolmogorov and Taylor micro scale for the shifted cases at the dynamical centreline ($x_s = 0$) and non-shifted cases at the geometrical centreline($x = 0$) for different Re_H. The Kolmogorov length scales are non-dimensionalised by using the inner (Figures 4 (a) and (b)) and outer (Figures 4 (c) and (d)) plume length scales for non-shifted and shifted cases. In figure 4 (b), the Kolmogorov length profiles collapse better in the region below $z/H = 0.2$ for shifted case for $L/H = 2$ and 4. Similarly, in figure 4 (d), we can observe that the profiles collapse in the region above $z/H = 0.2$ when non-dimensionalised by using the outer plume length scale.

The Baines and Turner's analytical solutions are compared with both shifted and non-shifted DNS results. Figures 5 (a) and (b) show the centreline vertical velocity profiles, and figures 5 (c) and (d) show the plume width calculated from the mean vertical velocity profile for shifted and non-shifted cases. The analytical solutions are obtained by using an entrainment coefficient $\alpha = 0.1$, which was found experimentally by Baines and Turner (1969) . In order to study the sensitivity of plume behaviour to plume length (L), we carried out simulations for three different length ($L/H = 1$, $L/H = 2$ and $L/H = 4$) for each Reynolds number (Re_H). The steady state results suggest that the plume lengths $L/H = 2$ and $L/H = 4$ are insensitive for the shifted case. Therefore, we fixed $L/H = 2$ for higher Re_H simulations. However, in non-shifted statistics for reduced gravity and vertical velocity profiles for $L/H = 2$ and $L/H = 4$, do not successfully collapsed at higher Re_H. The reduced gravity profiles (figures 5 (e) and (f)) show better agreement with the analytical results.

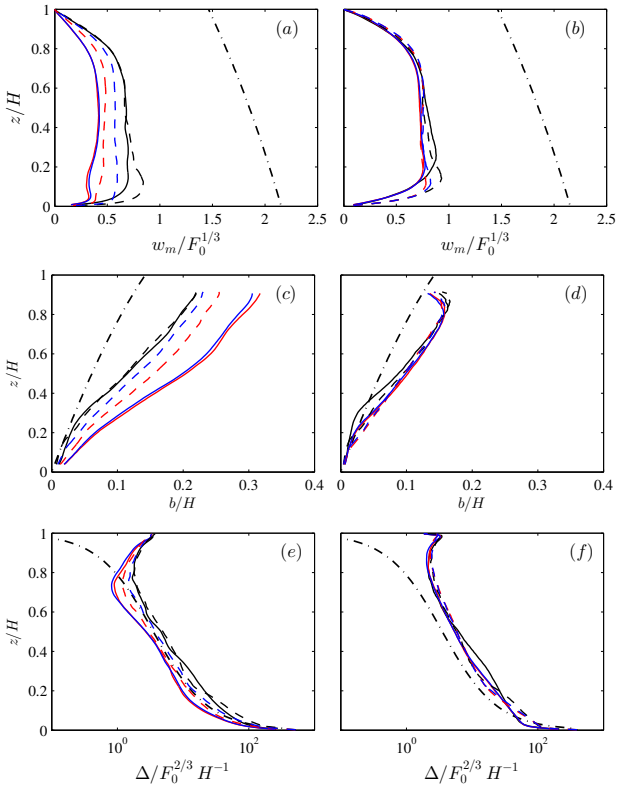

Figure 5: Comparison of vertical velocity, plume half width and reduced gravity profiles for non-shifted (a, c, e) at the geometrical centreline and shifted (b, d, f) at the dynamical centreline for different Re_H and L/H cases.; -·-·-·, $BT(1969)$; ——, $Re_H = 3840$($L/H = 1$); ——, $Re_H = 3840$ ($L/H = 2$); ——, $Re_H = 3840$ ($L/H = 4$); - - -, $Re_H = 7680$ ($L/H = 1$); - - -, $Re_H = 7680$ ($L/H = 2$) ; - - -, $Re_H = 7680$ ($L/H = 4$).

Conclusions

We have compared the Baines and Turner's analytical model with DNS for both shifted and non-shifted cases for two Reynolds numbers, 3840 and 7680; with plume lengths, $L/H = 1$, 2 and 4. The plume lengths $L/H = 2$ and $L/H = 4$ are found to be insensitive for the shifted cases. Overall, the reduced gravity profiles show good agreement with the theoretical predictions, although the maximum vertical velocity (w_m) is away from the analytical model.

Acknowledgements

The authors would like to gratefully acknowledge the financial support of the Bushfire and Natural Hazards Cooperative Research Council. This work was also supported by resources provided by the Pawsey Supercomputing Centre with funding from the Australian Government and the Government of Western Australia.

References

[1] Baines, W. D. and Turner, J. S., Turbulent buoyant convection from a source in a confined region, *J. Fluid Mech.*, **37**, 1969, 51–80.

[2] Cetegen, B. M., Dong, Y. and Soteriou, M. C., Experiments on stability and oscillatory behaviour of planar buoyant plumes, *Phy. Fluids.*, **10**, 1998, 1658–1665.

[3] Ng, C. S., Ooi, A., Lohse, D. and Chung, D., Vertical natural convection: application of the unifying theory of thermal convection, *J. Fluid Mech.*, **764**, 2015, 349–361.

[4] Hubner, J. 2004 Buoyant plumes in a turbulent environment. *Ph. D. Thesis*, Department of Applied Mathematics and Theoretical Physics, University of Cambridge, UK.

[5] Hunt, G. R., Cooper, P., and Linden, P. F. Thermal stratification produced by plumes and jets in enclosed spaces, *Building and Environment*, **36**, 2001, 871–882.

[6] Lee, S. L. and Emmons, H. S., A study of natural convection above a line fire. *J. Fluid Mech.*, **11**, 1961, 353–368.

[7] Paillat, S. and Kaminski, E., Entrainment in plane turbulent plumes. *J. Fluid Mech.*, **755**, 2014, R2.

[8] Morton, B. R., Taylor, G. I. and Turner, J. S. Turbulent gravitational convection from maintained and instantaneous sources, *Proc. R. Soc.*, A **234**, 1956, 1–23.

[9] Killworth, P.D. and Turner, J. S., Plumes with time-varying buoyancy in a confined region, *Geophys. Astrophys. Fluid Dyn*, **20**, 1982, 268–291.

[10] Kaye, N. B. and Hunt, G. R. Overturning in filling box, *J. Fluid Mech.*, **576**, 2007, 297–323.

[11] Zukoski, E. Fluid dynamics aspects of room fires, *Fire Safety Science*, **1**, 1986, 1–30.